

920555-1

OCTUPOLE CORRELATION EFFECTS IN NUCLEI

ANL/CP--75813

R. R. CHASMAN

DE92 018178

Physics Division, Argonne National Laboratory,
Argonne, IL 60439-4849

ABSTRACT

Octupole correlation effects in nuclei are discussed from the point of view of many-body wavefunctions as well as mean-field methods. The light actinides, where octupole effects are largest, are considered in detail. Comparisons of theory and experiment are made for energy splittings of parity doublets; E1 transition matrix elements and one-nucleon transfer reactions. The strong correlation picture that emerges from the many-body approach is found to provide a better description of octupole effects than does an octupole deformation picture.

1. Introduction

The presence of strong octupole correlations in deformed nuclei is signalled by dramatic changes in the nuclear excitation spectrum. In an even-even nucleus, the signature is a low-lying 1^- state. In an odd mass nucleus, the signature is a parity doublet. The parity doublet consists of a pair of states that have the same spin, opposite parities and are almost degenerate in energy. There should be a large E3 transition matrix element between the two states. In the octupole deformation limit, the 1^- state is between the 0^+ and 2^+ states of the ground state rotational band. In the odd mass case the members of the parity doublet would be degenerate in energy. In Fig. 1, we show idealized rotational spectra of nuclides with and without octupole deformation.

The first evidence for strong octupole correlation effects came from the discovery of low-lying 1^- states in alpha decay studies¹ of the light actinides by Asaro and co-workers. The 1^- states, near $A = 226$, are the lowest known excited states in even nuclei, apart from rotational excitations. In Fig. 2, we display the low-lying states of the Th isotopes. The low excitation energy of the 1^- states provides direct evidence for the presence of strong octupole effects in these nuclei. However, the fact that the 1^- state is never found below the 2^+ rotational state, and rarely below the 4^+ state, argues against ground state octupole deformation in even nuclides. The observation² by Kurcewicz et al., that the first 0^+ excited state in ^{224}Ra is at 916 keV, which is much more than twice the energy of the 1^- bandhead at 215 keV, suggests that a vibrational picture is not adequate to describe the strong octupole correlations in this region. Strong octupole correlation effects in odd mass nuclides were noted³ by Kroger and Reich in their study of the $3/2^+$ and $3/2^-$ bands of ^{229}Th .

Making use⁴ of variational many-body wavefunctions, we addressed the question of the effects of octupole correlations on the excitation energy of 0^+ excited states in the light actinides. We then examined⁵ the possibility of finding parity doublets in the odd mass nuclides of this region. This

The submitted manuscript has been authored by a contractor of the U. S. Government under contract No. W-31-109-ENG-38. Accordingly, the U. S. Government retains a nonexclusive, royalty-free license to publish or reproduce the published form of this contribution, or allow others to do so, for U. S. Government purposes.

MASTER

DISTRIBUTION OF THIS DOCUMENT IS UNLIMITED

calculation predicts the existence of many parity doublets in the light actinides, and their splittings, particularly a ground state parity doublet in ^{229}Pa .

Evidence for a ground state doublet was found at Argonne by Ahmad⁶ et al. More recent studies⁷ suggest that the experimental status of this doublet should be reinvestigated. It was also found⁸ that E1 transition rates are sometimes enhanced by several orders of magnitude in these nuclides, relative to values found near $A = 240$.

A later approach to the nuclides of this region is octupole deformation. Using the Strutinsky⁹ method, Moller and Nix¹⁰ found that the inclusion of octupole deformation gives ~ 1.5 MeV of extra binding energy in nuclides near $A \sim 222$. This brings the calculated binding energies into improved agreement with measured masses. Later studies^{11,12} have shown that this conclusion is modified substantially by the inclusion of higher deformation modes. The spectroscopic features of octupole deformation^{13,14,15} have been considered in detail by Leander and co-workers. This deformation picture gives many interesting relations between matrix elements in odd and even parity states. Hartee-Fock mean-field calculations using Skyrme¹⁶ and Gogny¹⁷ interactions have also been applied to studies of the light actinides.

3. Many-Body Wavefunctions

The many-body approach⁵ was the first to be used for treating octupole effects. The wave functions are sufficiently general that they can be used to describe the vibrational regime, the deformation regime, as well as the correlation regime intermediate between the two. The Hamiltonian that we use in these calculations is

$$H = H_{s.p.} + H_{\text{pairing}} + H_{\text{particle-hole}} \quad (1)$$

where

$$H_{\text{pairing}} = - \sum_{k,l} G_{k,l} A_k^+ A_{-k}^+ A_{-l} A_l \quad (1a)$$

The deformed single-particle energies of $H_{s.p.}$ were obtained from experimental studies of the heavier actinides, where octupole effects are not important. The pairing matrix elements are obtained from a density-dependent delta force interaction¹⁸, which was found to give a good description of the mid-actinide nuclides. The particle-hole interaction is of the multipole-multipole form and is restricted to $m = 0$ terms of the Legendre expansion, but can encompass all L values. In practice, we have included the octupole, 2^5 -pole and quadrupole multipoles. Our wavefunctions have a product form

$$\psi = \prod_z \left(\prod_{J_z} |J_z\rangle^T \right) \phi \left(\prod_z |J_z\rangle, \tau_z \right) \quad (2)$$

where each of the terms in the product is, in turn, a sum of many configurations. We have

$$\phi |J_z, \tau_z\rangle = \sum_i C_i \psi_i(|J_z, \tau_z\rangle) \quad (3)$$

where the sum includes all terms in the (j_z, τ_z) subgroup that have a specified value of J_z , including all values of parity and particle number. For the ground state of an even nucleus, we set $J_z = 0$ for each subgroup. To study the low-lying states of odd mass nuclides, we set $J_z = j_z$ in a single subgroup, fix the parity, and minimize the energy of the nucleus. Before determining the variational parameters, C_i , we project those configurations that have the desired particle number for both protons and neutrons and the desired overall parity. The variational parameters are obtained from the coupled, non-linear algebraic equations

$$\frac{\partial}{\partial C_i} \langle P(Np, Nn, \Pi) \psi | H | P(Np, Nn, \Pi) \psi \rangle = 0 \quad (4)$$

Using this structure for each of the subgroups, we can handle up to five doubly degenerate levels in each subgroup. By further factorizing¹⁹ the amplitudes, we reduce the number of variational parameters associated with each orbital and thereby can extend the space to include seven doubly degenerate levels in each subgroup. A separate calculation is carried out for the states of each parity and J_z . It is worth noting that parity projection prior to variation gives the same sort of improvement in wavefunctions, that one gets by number projection in the treatment of pairing interactions. As is the case for pairing, when the correlations are weak or of moderate strength, projection before variation is important. We further improve these wavefunctions by taking linear combinations of them. The additional solutions are obtained by taking the octupole interaction strength and the pairing strength as generator coordinates. In Figs. 3 and 4, we show the bandheads calculated with this approach for many of the states in odd-mass nuclides of this region. The numbers by the arrows are proportional to the squares of the E3 matrix elements between the states.

3. Octupole Deformation

The inclusion¹⁰ of octupole deformation in Strutinsky calculations gives a needed extra binding in the $A \sim 222$ mass region. This improves the agreement with measured masses; relative to calculations that include only quadrupole and hexadecapole deformation. Later studies¹¹ using the Strutinsky method showed that 2^6 pole deformations also play an important role in this region, and account for ~ 1 MeV of this extra binding. When 2^5 pole deformations are included¹², together with octupole deformation, one finds that the odd multipole deformation modes give ~ 1 MeV of extra binding relative to the reflection symmetric minimum. In the $A = 148$ mass region, these minima are found^{20,21} to be even shallower. In Fig. 5, we show qualitatively this difference in magnitude between octupole and

quadrupole deformed minima. In view of the fact that the 1^- state is always well above the 2^+ state in all nuclides (and that the fact that barriers between reflection symmetric and asymmetric shapes are about 1 MeV), one can infer that barriers of at least 1.5 - 2 MeV are necessary for a deformation picture to hold. In odd mass nuclides, the octupole deformed description# gives predictions of parity doublets and many relations between matrix elements. Magnetic moments are predicted to be equal^{13,14} and decoupling parameters in $K = 1/2^\pm$ bands are equal in magnitude²² but opposite in sign. Transition probabilities between the levels of two doublets should also be identical. By analyzing the single-particle wavefunctions^{23,15} in terms of spherical components, it is possible to make predictions of one-particle transfer cross-sections to the members of an octupole deformed rotational band; which encompasses states of both even and odd parity. The mixed parity single particle wavefunctions, that are high J, and unique parity in the reflection symmetric limit are admixed with low J states of opposite parity, and this nicely explains²⁴ the reduction in alignment that is seen in the $A = 220$ mass region.

4. Studies of ^{229}Pa and ^{227}Ac

The effects of octupole correlations are more apparent in odd mass nuclides than in even-even nuclides, because of pairing interactions. The positive parity ground state band of an even nuclide has no broken pairs, while all configurations that have negative parity have at least one broken pair. This implies a shift in energy of the odd parity states relative to the even ones. In an odd mass nuclide, the situation is quite different. Both members of the parity doublet must have at least one unpaired particle, and the situation is equivalent for states of both parities. Further, the reduction in pairing strength arising from the level blocking of the unpaired nucleon makes it easier for the octupole correlations to develop. The squared $E3$ matrix elements, that are typically 50 units in the even nuclides, can be⁵ as large as 90 units in the odd mass nuclides.

We can illustrate most of these effects by considering the two nuclides, ^{229}Pa and ^{227}Ac in detail. In Fig. 6 the theoretical and experimental treatments of ^{229}Pa are shown as a function of time. In Fig. 7, we show a similar figure for ^{227}Ac . The prediction⁵ of a ground state parity doublet with a spin of $5/2$ in ^{229}Pa motivated the experimental⁶ studies. Definitive evidence was found for a ground state spin assignment of $5/2$, and strong evidence for a ground state parity doublet. Recent studies⁷ of Grafen et al. have reopened the question of a ground state doublet and this question is being reinvestigated. Combining gamma ray data from both experiments suggests that the $1/2^-$ band is ~ 35 keV from ground²⁶; in rather good agreement with the original predictions. The fact that the ground state band is $K = 5/2$ in this nuclide, rather than $K = 1/2$, as is the case in ^{231}Pa , is due to the strong octupole correlations.

The data in ^{227}Ac are more extensive, as this nuclide is easier to produce. In addition to spin assignments, there are one-particle transfer data and observed decoupling parameters. It should be noted that there is

no shifting of levels in the octupole deformed calculations of Ref. 25. In Fig. 8, we show the comparison of structure factors measured²⁷ in (⁴He,t) and (³He,d) reactions with the predictions of reflection symmetric and reflection asymmetric potentials. It is quite clear that the reflection symmetric potential is in considerably better agreement with the data for most levels. The disagreements between the experimental data and the reflection asymmetric picture in the peaks of the 1/2⁺ and 1/2⁻ bands tells us immediately that the octupole deformed model does not give the decoupling parameters of these bands correctly, as the decoupling parameters are simply related to the structure factors by

$$a = \sum_j (-1)^{j-1/2} C_j^2 \quad (5)$$

In Table 1, we compare calculated and measured decoupling parameters in this nucleus.

Table 1. Decoupling Parameters in ²²⁷Ac

	No Octupole a)	Octupole a)	Many-Body b)	Expt.c)
1/2 ⁺	5.92	3.13	4.9	4.8
1/2 ⁻	-1.76	3.13	-2.1	-2.2

a) Ref. 14

b) R. R. Chasman, Nuclear Structure, Reactions and Symmetries, p. 5, ed. R. A. Meyer and V. Paar (World Scientific, Singapore, 1986)

c) A. K. Jain et al., Rev. Mod. Phys. **62** (1990) 393.

The many-body model provides a better description than does the deformation picture. It should be noted that the octupole deformation picture does provide a good description of the g_k factors for the 3/2⁺ and 3/2⁻ bands in this nucleus. In the absence of octupole correlations, the calculated values¹⁴ are 0.50 for the 3/2⁻ band and 1.50 for the 3/2⁺ band; while the calculated values are 0.89 for both bands in the octupole deformation limit. Experimentally, both bands are found to have g_k values of ~0.95. It is, therefore, somewhat troublesome that the reflection asymmetric model does such a poor job of fitting the transfer data for these two 3/2 bands.

5. E1 Transition Matrix Elements

5. E1 Transition Matrix Elements

In the early studies⁸ of the light actinides, several cases of large E1 transition matrix elements were found. In Fig. 9, we show $T(E1)$ values for several nuclides in this region. The important points are: (1) that there are several cases where the $T(E1)$ values are extremely large, in the region of strong octupole correlations; (2) equally important, there are variations of two orders of magnitude in this region.

The relation between the phases of the E3 and E1 transition matrix elements connecting two states is that the two are usually in phase when the E3 and E1 matrix elements are large. Also, transitions with large E3 matrix elements tend to have large E1 matrix elements. This means that when one has e.g. a coherent sum for the E3 proton matrix elements, there is also a coherent sum for the E1 proton matrix elements. The difference between the two is that the E3 transition is isovector and the E1 transition is isoscalar. The proton and neutron contributions to the E3 transition are in phase because the proton-neutron octupole-octupole term in the residual interaction is attractive. The form of the E1 matrix element is

$$B(E1) = \langle \psi^+ | (E1)_{\text{proton}} - (Z/N) (E1)_{\text{neutron}} | \psi^- \rangle^2 \quad (6)$$

where

$$(E1)_{\text{proton}} = \sum_{\text{proton orbitals } i,j} \langle i | \langle \gamma_1^0 | j \rangle A_i^+ A_j \quad (6a)$$

and there can be large cancellations between the proton and neutron contributions to the E1 transition.

The first serious efforts²⁸ to calculate these E1 matrix elements were made in the framework of the Strutinsky method. In this framework, the E1 matrix element is given as

$$B(E1) = \left[\left[\frac{1}{3.6} \langle \psi^\pm | ((E1)_p - (\tilde{E}1))_{\text{psot}} - Z/N (E1 - \tilde{E}1)_{\text{neutron}} | \psi^\pm \rangle + (E1)_{\text{liquid drop}} \right] \right]^2 \quad (7)$$

There, it was found that such calculations must be adjusted to account for the fact that the deformed Woods-Saxon potentials used to generate energy levels and matrix elements do not include in any way the depletion of E1 strength that is absorbed by the isovector giant dipole resonance. This depletion is treated in an average way by reducing the shell contributions to the E1 moment by a factor of 3.6, i.e. an order of magnitude in transition probability. Additionally, it was found that the liquid drop contribution to the E1 moment must be reduced about 15% from the conventional value, in order to get a good fit to the data. However, using a standard set of parameters for the droplet model, it was pointed out²⁹ that there is a neutron skin contribution to the liquid drop E1 moment that is comparable in magnitude and opposite in sign to the charge

redistribution effect, giving an order of magnitude reduction to the liquid drop E1 moments posited in Ref. 28. Recently, it has been noted³⁰, that the droplet parameters can be readjusted within acceptable limits, to give droplet correction to the E1 probabilities of the needed magnitude. In any event, this approach to the calculation of E1 moments should be regarded as a two parameter theory that does reasonably well.

Quite recently, E1 matrix elements have been obtained³¹ in a microscopic calculation with parity projection. The calculation is done with a standard Gogny force, which does give a reasonable treatment of the giant dipole. There are no adjustable parameters here and the results are in good agreement with measured E1 values. In Fig. 10, we compare the values of Q_1^2 calculated for the Ra isotopes with experimental³² studies. The no free parameter Gogny interaction seems to be doing a better job than the two-parameter shell correction approach. It remains to be seen if the large E1 moments that are calculated for ^{228}Ra and ^{230}Ra , with the Gogny force, are confirmed by experiment.

6. Summary

The octupole degree of freedom is manifested in a dramatic way in nuclear spectra, particularly in the light actinides. Here the octupole correlations are strong, but not sufficiently strong to be described accurately by a simple deformation description. The deformation approach does, however, provide a very useful qualitative insight into many octupole phenomena, and provides surprisingly accurate results in many instances. The many-body approach, that puts the pairing and particle-hole modes on an equal footing, provides a somewhat better picture of this region.

I thank I. Ahmad for many interesting and illuminating discussions on the subject of octupole correlations. Some of the calculations discussed here were carried out on the NERSC computer facility. This research was supported by the U.S. Department of Energy, Nuclear Physics Division, under contract W-31-109-ENG-38.

DISCLAIMER

This report was prepared as an account of work sponsored by an agency of the United States Government. Neither the United States Government nor any agency thereof, nor any of their employees, makes any warranty, express or implied, or assumes any legal liability or responsibility for the accuracy, completeness, or usefulness of any information, apparatus, product, or process disclosed, or represents that its use would not infringe privately owned rights. Reference herein to any specific commercial product, process, or service by trade name, trademark, manufacturer, or otherwise does not necessarily constitute or imply its endorsement, recommendation, or favoring by the United States Government or any agency thereof. The views and opinions of authors expressed herein do not necessarily state or reflect those of the United States Government or any agency thereof.

References

1. F. Asaro and I. Perlman, *Phys. Rev.* **104** (1956) 91.
2. W. Kurcewicz et al., *Nucl. Phys.* **A289** (1977) 1.
3. L. A. Kroger and C.W. Reich, *Nucl. Phys.* **A259** (1976) 29.
4. R. R. Chasman, *Phys. Rev. Lett.* **42** (1979) 630.
5. R. R. Chasman, *Phys. Lett.* **B96** (1980) 7.
6. I. Ahmad et al., *Phys. Rev. Lett.* **49** (1982) 1758.
7. V. Grafen et al., *Phys. Rev.* **C44** (1991) 1728.
8. I. Ahmad et al., *Phys. Rev. Lett.* **52** (1984) 503.
9. V. M. Strutinsky, *Nucl. Phys.* **A95** (1967) 420.
10. P. Moller and J. R. Nix, *Nucl. Phys.* **A361** (1981) 117.
11. R. R. Chasman, *Phys. Lett.* **B175** (1986) 254.
12. A. Sobiczewski et al., *Nucl. Phys.* **A485** (1988) 16.
13. G. A. Leander et al., *Nucl. Phys.* **A388** (1982) 452.
14. R. K. Sheline and G. Leander, *Phys. Rev. Lett.* **51** (1983) 359.
15. G. A. Leander and Y. S. Chen, *Phys. Rev.* **C37** (1988) 2744.
16. P. Bonche et al., *Phys. Lett.* **B175** (1986) 387.
17. L. M. Robledo et al., *Phys. Lett.* **B187** (1987) 223.
18. R. R. Chasman, *Phys. Rev.* **C14** (1976) 1935.
19. R. R. Chasman, *Phys. Lett.* **B219** (1989) 232.
20. S. Cwiok and W. Nazarewicz, *Nucl. Phys.* **A496** (1989) 367.
21. J. L. Egido and L. M. Robledo, *Nucl. Phys.* **A518** (1990) 475.
22. I. Ragnarsson, *Phys. Lett.* **B130** (1983) 353.
23. R. R. Chasman, *Phys. Rev.* **C30** (1984) 1753.
24. W. Nazarewicz et al., *Phys. Rev. Lett.* **52** (1984) 1272.
25. S. Cwiok and W. Nazarewicz, *Nucl. Phys.* **A529** (1991) 95.
26. I. Ahmad (private communication).
27. H. E. Martz et al., *Phys. Rev.* **C37** (1988) 1407.
28. G. A. Leander et al., *Nucl. Phys.* **A453** (1986) 58.
29. C. O. Dorso et al., *Nucl. Phys.* **A451** (1986) 189.
30. P. A. Butler and W. Nazarewicz, *Nucl. Phys.* **A533** (1991) 249.
31. J. L. Egido and L. M. Robledo, *Nucl. Phys.* **A524** (1991) 65.
32. R. J. Poynter et al., *Phys. Lett.* **B232** (1989) 447.

Figure Captions

- Figure 1: Idealized Rotational Spectra without and with Octupole Deformation.
- Figure 2: Excitation Energies of 1^- , 2^+ and 4^+ States in the Th Isotopes.
- Figure 3: Many-Body Calculation of Bandheads in Odd-proton Nuclei. The numbers beside the arrows are proportional to the squares of the $E3$ matrix elements. The % denotes levels known at the time of the calculation.

- Figure 4: Many-Body Calculation of Bandheads in Odd-neutron Nuclei. See caption for Fig. 3.
- Figure 5: Calculation of Typical Binding Energy gains for Quadrupole and Octupole Deformation obtained with the Strutinsky Method. The deformation axis is e_2 for the quadrupole case and e_3 for the octupole case. The gain in binding energy for the octupole is relative to the reflection symmetric minimum.
- Figure 6: Experimental and Theoretical Bandheads in ^{229}Pa . The spectra are time ordered, with the earliest on the left. Bold lines are used for experimental spectra. (a) Ref. 5: (b) Ref. (6): (c) Ref. (15): (d) Ref.'s (7) and (26): (e) Ref. (25).
- Figure 7: Experimental and Theoretical Bandheads in ^{227}Ac . See caption for Fig. 7. (a): Table of Isotopes, C. M. Lederer et al. (John Wiley and Sons, New York, 1978): (b) Ref. 5: (c) Ref. 14: (d) Ref. 27: (e) Ref. 15: (f) Ref. 25.
- Figure 8: Comparison of Experimentally measured Structure Factors with Reflection Symmetric and Reflection Asymmetric Calculations.
- Figure 9: E1 Transition Rates in Weisskopf Units.
- Figure 10: Comparison of Experimental and Theoretical E1 Transition Probabilities.

$$\left(\frac{3}{4\pi}\right) Q_1^2 \langle I, K, 1, 0 | I^1, K^1 \rangle^2$$

The squares are the experimental points given in Ref. 32. The diamonds are the calculations of Ref. 31. The circles are the calculations of Ref. 28.

QUADRUPOLE DEFORMATION

QUADRUPOLE + OCTUPOLE DEFORMATION

EVEN ODD

EVEN ODD

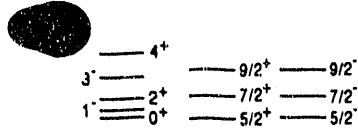
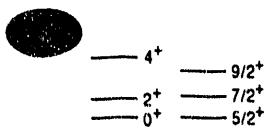


Fig. 1

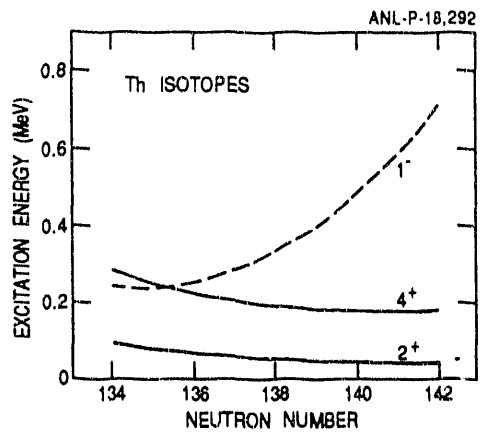


Fig. 2

ANL-P-18,290

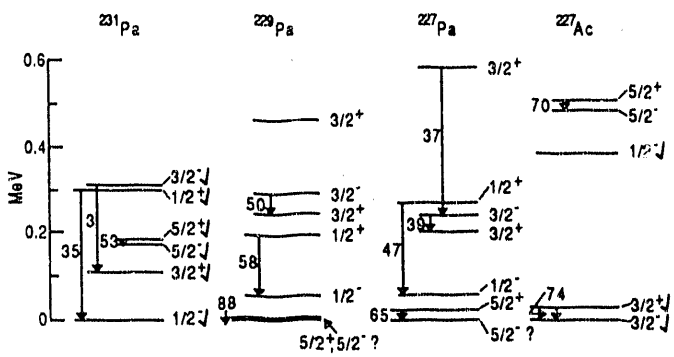


Fig. 3

ANL-P-18,201

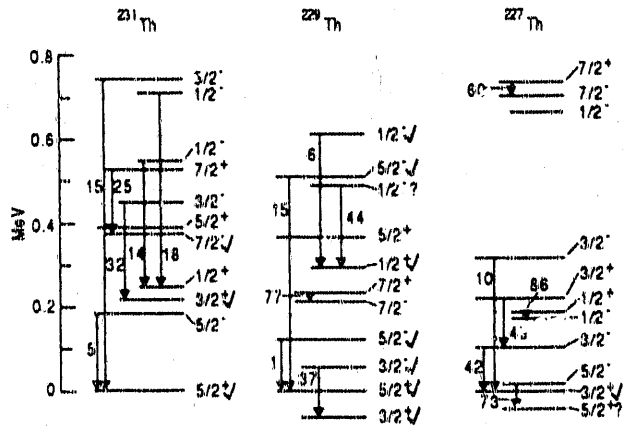


Fig. 4

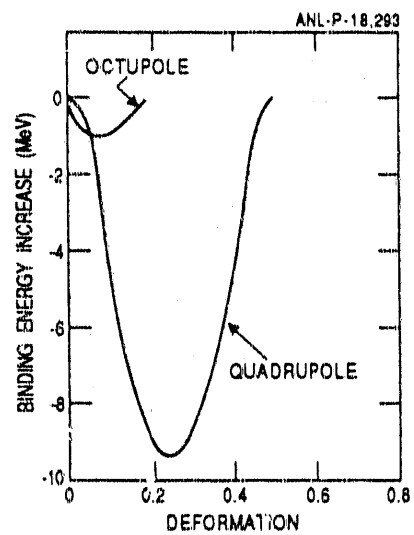


Fig. 5

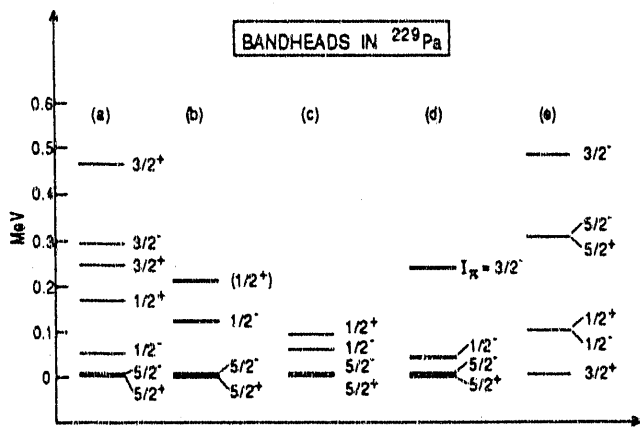


Fig. 6

Fig 6

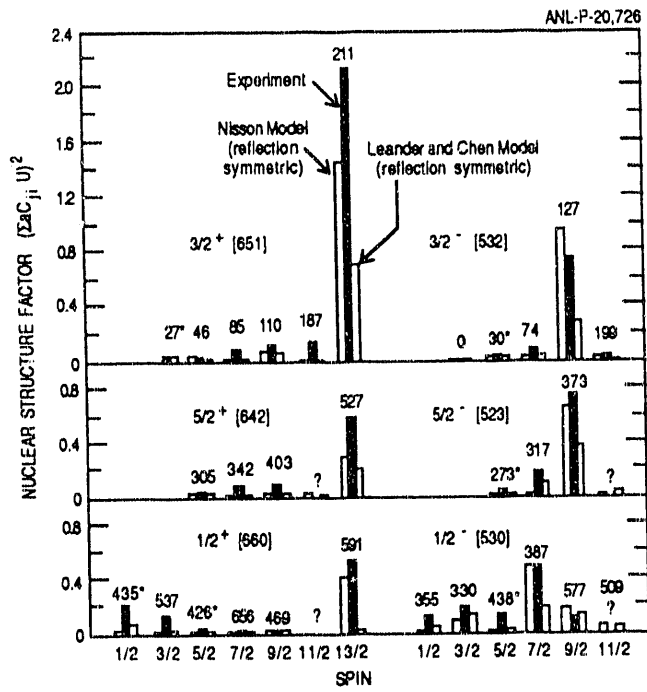


Fig. 8

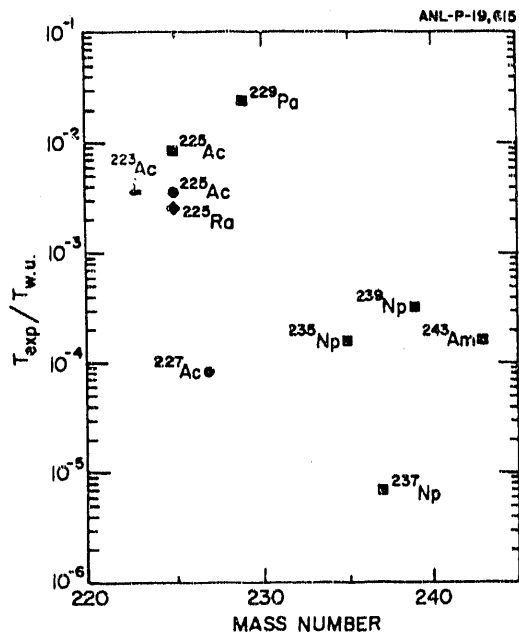


Fig. 9

Fig 9

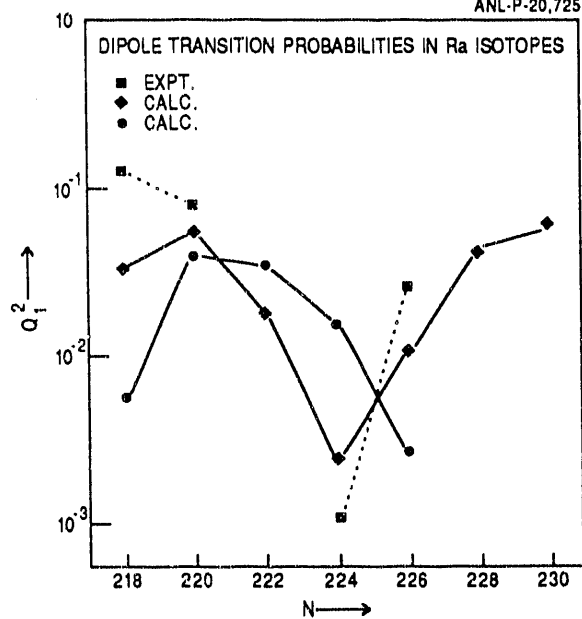


Fig. 10

Fig 10

**DATE
FILMED**

8/3/92

